[CANCER RESEARCH 61, 4827–4836, June 15, 2001]

Fragile Histidine Triad Expression Delays Tumor Development and Induces Apoptosis in Human Pancreatic Cancer[1]

Kristoffel R. Dumon,[2] Hideshi Ishii,[2] Andrea Vecchione, Francesco Trapasso, Gustavo Baldassarre, Fatima Chakrani, Teresa Druck, Ernest F. Rosato, Noel N. Williams, Raffaele Baffa, Matthew J. During, Kay Huebner, and Carlo M. Croce[3]

Kimmel Cancer Center, Thomas Jefferson University [K. R. D., H. I., A. V., F. T., G. B., F. C., T. D., R. B., M. J. D., K. H., C. M. C.], and Department of Surgery, Hospital of the University of Pennsylvania [K. R. D., E. F. R., N. N. W.], CNS Gene Therapy Center, Department of Neurosurgery, Jefferson Medical College, Philadelphia, Pennsylvania 19107

ABSTRACT

The *fragile histidine triad* (*FHIT*) gene is a tumor suppressor gene that is altered by deletion in a large fraction of human tumors, including pancreatic cancer. To evaluate the potential of *FHIT* gene therapy, we developed recombinant adenoviral and adenoassociated viral (AAV) *FHIT* vectors and tested these vectors *in vitro* and *in vivo* for activity against human pancreatic cancer cells. Our data show that viral *FHIT* gene delivery results in apoptosis by activation of the caspase pathway. Furthermore, Fhit overexpression enhances the susceptibility of pancreatic cancer cells to exogenous inducers of apoptosis. *In vivo* results show that *FHIT* gene transfer delays tumor growth and prolongs survival in a murine model mimicking human disease.

INTRODUCTION

Pancreatic cancer remains one of the most difficult malignancies to treat. It ranks fourth as a cause of cancer-related deaths in the United States and accounts for an estimated 29,000 deaths yearly (1). Pancreatic cancer, 85% of which is of ductal cell origin, has a negligible 5-year survival rate (1.3%), which is the lowest rate among 60 cancer sites reviewed (2). Currently, radiation and chemotherapy are not effective, and complete surgical resection remains the only therapeutic option. Although surgery provides a limited potential for long-term survival, only 5% of tumors are resectable at the time of diagnosis. In addition, for all stages of surgically resectable disease combined, the overall 5-year survival is <15% (3). Therefore, there is urgent need of alternative therapeutic strategies.

The molecular dissection of pancreatic cancer is progressing at a rapid pace. Activation of oncoproteins such as K-ras and inactivation of tumor suppressors such as p53, p16, p21/WAF, and Fhit are involved in the development of pancreatic cancer (4–8). The translation of these findings into therapeutic modalities is emerging. Immune gene therapy (9) and adenovirus-based *p21* and *p53* gene transfer are part of such strategies currently explored as potential gene therapy approaches for pancreatic adenocarcinoma (10, 11).

A considerable amount of data support the suggested role of the *FHIT*[4] gene, at chromosome 3p14.2, as a tumor suppressor gene in different epithelial cancers (reviewed in Ref. 12). For human pancreatic cancer, studies indicate that *FHIT* is affected in ~66% of cell lines and surgical specimens (7, 13), comparable with TP53, which is mutated in approximately 43–76% of primary pancreatic cancers (5).

Virus-mediated *FHIT* gene transfer has been shown to induce apoptosis and reduce tumor growth in epithelial cancers such as esophageal and lung cancer (14, 15), but the effect of *FHIT* transduction in human pancreatic cancers is not known. Recent evidence from transfection of human lung cancer cells with *FHIT* are consistent with its involvement in p53-independent apoptosis (14, 16). This could be of particular interest in the treatment for pancreatic cancer, because transduction of wild-type p53 into p53-null human pancreatic cancers sometimes failed to induce changes in tumorigenicity and chemosensitivity (11).

We hypothesized that reintroduction of a wild-type human *FHIT* gene, mediated by a recombinant viral vector, would result in cell cycle delay, induction of apoptosis, and tumor growth suppression in *FHIT* null pancreatic cancer cells. A number of recombinant viral vector systems are currently under evaluation for gene therapy in cancer. Adenoviral vectors are probably the most widely used vectors for human cancer gene therapy (17). Adenoviral vectors are very efficient in delivering genes into pancreatic cancer cells. They induce high but transient transgene expression. They have also been reported to induce inflammatory responses in animal models and patients (18, 19). These side effects have been attributed to the leaky expression of the residual viral genes carried by the vectors and might ultimately limit their clinical use.

AAV viruses, which to our knowledge have not been studied in human pancreatic cancer, have specific features that render them attractive for human applications. Epidemiological studies indicate that 90% of the human population has been exposed to AAV with no known associated pathologies. In addition to the nonpathogenic nature, other major advantages of AAV include: (*a*) infection of nondividing cells; (*b*) persistent gene expression through integration into the cellular chromosomes or by conversion into double-stranded episomal forms; (*c*) delivery of the therapeutic gene without cotransfer of any viral genes; and (*d*) natural tropism for epithelial cells (20–22). This allows the transgene to persist in the target tissue and renders AAV vectors unlikely to induce inflammatory responses against the transduced cells. Experiments with recombinant AAV-mediated gene transfer into skeletal muscles and other tissues, for example kidney (23), have shown persistent transgene expression with no inflammatory responses in animal models and primates (24–26). Although the difficulty of high-titer rAAV vector production has overshadowed its potential benefits, recent advances in the production of high-titer purified rAAV vector stocks have made the transition to human clinical trials a reality (22). In this study, we generated both Ad FHIT vectors (Ad-FHIT) and rAAV vectors for FHIT (AAV-FHIT) and explored their use as *FHIT* gene transfer vehicles into pancreatic cancer.

MATERIALS AND METHODS

Cell Cultures. Human pancreatic cancer cell lines AsPc1, HPAF, BxPc3, Panc1, Hs766T, Capan1, Capan2, MiaPaca, and CFPAC; the human cervical

Received 2/2/01; accepted 5/2/01.

The costs of publication of this article were defrayed in part by the payment of page charges. This article must therefore be hereby marked *advertisement* in accordance with 18 U.S.C. Section 1734 solely to indicate this fact.

[1] This study was supported by Grants P01-CA77738 and CCSG P30-CA56036 (to K. H. and C. M. C.). K. R. D. is supported by Postdoctoral Research Fellowship F32 CA86429-01 from the National Cancer Institute. This study would not have been possible without the generous support of George Strawbridge.

[2] These authors contributed equally to this study.

[3] To whom requests for reprints should be addressed, at Kimmel Cancer Center, Jefferson Medical College, 233 South 10th Street, Philadelphia, PA 19107. E-mail: c_croce@lac.jci.tju.edu.

[4] The abbreviations used are: FHIT, fragile histidine triad; AAV, adenoassociated viral; rAAV, recombinant AAV; Ad, adenoviral; GFP, green fluorescent protein; EF, elongation factor; MOI, multiplicities of infection; FACS, fluorescence-activated cell sorting; PI, propidium iodide; LM-PCR, ligation-mediated PCR; PARP, poly(ADP-ribose) polymerase; PFU, plaque-forming unit; TNF, tumor necrosis factor; HSPG, heparan sulfate proteoglycan.

Downloaded from http://aacrjournals.org/cancerres/article-pdf/61/12/4827/2486769/4827.pdf by guest on 24 August 2022

epithelial cancer cell line, HeLa; the human lung cancer cell line A549; and human embryonic kidney cells (HEK293) were obtained from American Type Culture Collection. PSN1 was obtained from the European Collection of Cell Cultures. Cells were maintained at 37°C in a humidified atmosphere of 5% CO_2 in the appropriate growth medium with supplements added as recommended (15, 27, 28). The 293 cell line was used for the construction and amplification of both Ad and AAV vectors.

Construction of Recombinant Ad Viral Vectors. We generated an adenovirus carrying the *FHIT* gene (Ad-FHIT) under the control of a cytomegalovirus promoter by homologous recombination in 293 cells. The same procedure was used to generate an adenovirus containing GFP (Ad-GFP). Also, an Ad vector with simultaneous expression of GFP and FHIT through an internal ribosomal entry site was constructed by the same procedure (Ad-GFP-FHIT). Vector construction was performed following the manufacturer's instructions (Quantum, Quebec, Canada) with minor modifications, as described previously (15). Viral vectors were amplified in 293 cells, and viral titers were determined by assay for PFUs. Potential contamination of the viral preparation by the wild-type virus was monitored by PCR analysis.

Construction and Generation of Recombinant AAV. For the production of AAV vectors, we constructed two recombinant AAV type 2 vectors packaged with FHIT and GFP, respectively. The FHIT and GFP cDNA was inserted into the vector plasmid *pAM/pL-EF-GFP-WPRE-BGHpolyA*. For packaging, we used the helper plasmid *pDG*, which contains all AAV and Ad functions, including the *rep* and *cap* genes required for amplification and packaging of AAV vector plasmids (29).

The plasmid *AAV/EF-GFP-WPRE-poly(A)*, carrying the AAV-ITR and the EF promoter, was purified and digested with restriction enzymes *Kpn*I and *Hin*dIII to release a fragment containing the promoter sequence EF controlling the reporter gene GFP. The EF-GFP fragment was cloned into the *Kpn*I and *Hin*dIII restriction sites of the multiple cloning site of *pAM/pL-WPRE-BGH-poly(A)*, creating *pAM/pL-EF-GFP-WPRE-BGH-poly(A)*. The plasmid pIRES FHIT was purified and digested with restriction enzymes to release the 444-bp fragment containing the full-length *FHIT* gene. Subsequently, FHIT cDNA was cloned into the *Bam*HI and *Hin*dIII sites of *pAM/pL-EF-GFP-WPRE-BGH-poly(A)*, replacing GFP with FHIT to generate *pAM/pL-EF-FHIT-WPRE-BGH-poly(A)*. The plasmids *pAM/pL-EF-FHIT-WPRE-BGH-poly(A)*, *pAM/pL-EF-GFP-WPRE-BGH-poly(A)*, and the AAV-helper plasmid *PDG* were selected, amplified, and purified in large quantities. Helper-free recombinant AAV stocks were generated by cotransfection of the vector plasmids with the packaging plasmid *pDG* in 293 cells to obtain AAV-GFP and AAV-FHIT. Virus purification and titration was performed as described previously (29). After viral purification, slot blot analysis was performed to determine the concentration of AAV-FHIT and AAV-GFP. The viral titer was determined to be 1×10^{11} to 1×10^{12} particles/ml by comparing the similarly intense bands in the control lane to those on the AAV-GFP and AAV-FHIT lanes, corresponding to 10^9 to 10^8 infectious particles/ml.

***In Vitro* Transduction.** For Ad vectors, cells (1×10^6/well for six-well plates, 5×10^5/well for 12-well plates, 1×10^5/well for 48-well plates, and 0.5×10^5/well for 96-well plates) were transduced with Ad vectors by directly applying the diluted viruses into the growth medium. Cells were infected with the various viruses at different MOI. The transduction efficiency was determined by measuring the proportion of GFP-expressing cells after Ad-GFP infection using FACS. Direct visualization of the Ad-GFP-transduced cell population by fluorescent cell microscopy was used to confirm the FACS data.

For AAV vectors, cells were seeded at the same cell density as for Ad vectors. The human cervical cancer cell line, HeLa, known to be highly permissive for AAV infection, was used as a reference cell line to optimize *in vitro* conditions. Prior to infection, cells were treated with 500 μM tyrphostin 1 (Sigma Chemical Co., St. Louis, MO) for 2 h at 37°C. Tyrphostin 1 is a fibroblast growth factor receptor protein tyrosine kinase, known to augment AAV-mediated *in vitro* transgene expression (30). After treatment, cells were washed twice with PBS and were either mock infected or infected with 10^4 to 10^5 viral particles/cell of the recombinant AAV-GFP virus in DMEM supplemented with 10% FBS and analyzed by FACS and confocal microscopy to determine the transduction efficiency.

Assessment of *in Vitro* Cell Death. Cells were infected with AAV-FHIT and AAV-GFP at different viral concentrations or mock-infected with PBS. Similarly, cells were infected with Ad-FHIT and Ad-GFP at different MOI or mock-infected with PBS and harvested at different time points after infection.

To determine the percentage of dead cells, cells were stained with 0.2% trypan blue and counted with a hemocytometer. As a measurement of the fraction of apoptotic cells, the following methods were used. The fraction of hypodiploid cells was determined by FACS analysis after staining with PI, DNA fragmentation was measured by APO-BRDU (PharMingen, San Diego, CA), DNA laddering was evaluated by LM-PCR (Clontech, Palo Alto, CA), and ApoAlert Mitochondrial Membrane Sensor (Clontech, Palo Alto, CA) was used in fluorescence-based detection of changes in mitochondrial membrane potential.

Analysis of Cell Cycle by PI Staining and Measurement of DNA Fragmentation by Bromodeoxyuridine Labeling. DNA fragments in apoptotic cells were detected with an APO-BRDU kit (PharMingen), according to the manufacturer's instructions. Briefly, 10^5 cells were harvested 5 days after infection and washed twice with PBS. Cells were fixed in 1% formaldehyde for 15 min at 4°C, permeabilized in 500 μl of 70% ethanol, and stored at 4°C. Then, the 3′-hydroxyl ends of the DNA fragments in apoptotic cells were labeled with bromodeoxyuridine triphosphate by terminal deoxynucleotidyltransferase, and bromodeoxyuridine triphosphate was stained with a FITC-labeled anti-bromodeoxyuridine monoclonal antibody. Cells were simultaneously stained with PI. Analysis of cell populations was performed with FACScan. Cells were analyzed for green FITC fluorescence through a 520-nm BP filter and for red (PI) fluorescence through a 620-nm LP filter. Green fluorescence was taken as a marker of DNA fragmentation and apoptosis, red fluorescence was taken as a marker of DNA content and cell cycle status. Cells with subdiploid DNA content (sub-G_1) were considered apoptotic cells. Cell cycle distributions were analyzed by the Win MDI 2.8 software package.

Analysis of Cell Surface Markers. In separate experiments, approximately 5×10^5 cells of each cell line were washed with PBS at 4°C and incubated with 10 μg/ml of the following antibodies: anti-integrin $\alpha V\beta 3$, anti-integrin $\alpha V\beta 5$ (clones LM609 and P1F6; Chemicon, Temecula, CA), anti-HSPG (clone MAB458; Clontech), and anti-fibroblast growth factor receptor monoclonal antibody (Zymed, South San Francisco, CA), and analyzed by FACS.

Detection of DNA Laddering by LM-PCR. Five days after infection with different viruses (AAV-GFP, AAV-FHIT, and mock), DNA from the pancreatic cancer cell line, Panc1, and the lung cancer cell line, A549, was extracted. We used 0.75 μg of DNA for each reaction and followed the protocol provided by the manufacturer for the ApoAlert LM-PCR Ladder Assay. As a thermostable DNA polymerase, we used Advantage cDNA Polymerase Mix (Clontech). The resulting nucleosomal ladder was visualized on a 1.4% agarose/ethidium bromide gel.

Cell Staining with MitoSensor. After infection with different viruses (Ad-GFP, Ad-FHIT, and mock), cells were stained with the Mitosensor reagent following the manufacturer's instructions (Clontech). The Mitosensor reagent is taken up in the mitochondria of healthy cells, where it forms aggregates that exhibit red fluorescence. In apoptotic cells, MitoSensor remains in the cytoplasm in monomeric form, where it exhibits green fluorescence. Bisbenzimide (Hoechst Blue, 1 μg/ml in PBS; Sigma Chemical Co.) was used as a nuclear blue stain. Cells were visualized by fluorescence microscopy using a triple band-pass filter.

Western Blot Analysis. Cell lysates were prepared as described (16), and Western blots were performed by using 50 μg of total proteins/lane. Protein samples were electrophoresed on 4–20% SDS-polyacrylamide gels and transferred to nitrocellulose filters, and filters were incubated with the indicated antisera. Immunoreactive bands were visualized by using horseradish peroxidase-conjugated secondary antiserum and enhanced chemiluminescence (Amersham, Piscataway, NJ). For Western blot analysis, we used rabbit polyclonal Fhit antibody at 1:1000 (Zymed), rabbit polyclonal caspase-8 antibody at 2 μg/ml (Chemicon), PARP monoclonal antibody at a 1:5000 dilution (Clontech), rabbit polyclonal caspase-3 antibody at a 1:1000 dilution (PharMingen), rabbit polyclonal caspase-9 antibody at a dilution of 1:500 (Santa Cruz Biotechnology), goat polyclonal BID antibody at a dilution of 1:500 (Santa Cruz), and anti-actin at 1:2000 (Sigma Chemical Co.).

Immunohistochemistry. After antigen retrieval, endogenous peroxidase was inhibited with 3% hydrogen peroxide, and nonspecific binding sites were blocked with normal goat serum. Slides were incubated overnight with primary rabbit antihuman Fhit antibody (1:1000 dilution; Zymed), followed by incubation with biotinylated goat antirabbit antibody. Slides were then incubated with streptavidin horseradish peroxidase (Dako; 1:1000 dilution).

Downloaded from http://aacrjournals.org/cancerres/article-pdf/61/12/4827/2486769/4827.pdf by guest on 24 August 2022

Culture Conditions for External Stimulation Assays. Cells (PSN1 and Panc1) were plated at 1×10^5 cells/well in 48-well plates and infected under three conditions (Ad-GFP-FHIT, Ad-GFP, and mock) at MOI of 10 for Panc1 and at MOI of 20 for PSN1. Ad-GFP was used to control transduction levels. At these MOI, these cell lines were known to exhibit apoptosis in ~20% of the cells. Experiments were conducted in triplicate. After 3 days, cells were incubated with three different external stimuli: human Fas ligand (0.5 μg/50 μl of CD95NA/LE; clone DX2; PharMingen; and 0.5 μg/50 μl rProtG in 200 μl of 10% FBS medium); IFN-γ (200 units/ml; R&D Systems, Minneapolis, MN); or TNF-α (1000 units/ml; R&D Systems). After 12 h incubation at 37°C, cells were harvested. Cell count and cell cycle analysis were performed as described. Susceptibility of Ad-GFP-FHIT-infected cells was compared with Ad-GFP and mock-infected controls.

Animal Studies. Animals were maintained and animal experiments conducted under institutional guidelines established for the Animal Facility at the Kimmel Cancer Center. *nu/nu* mice were obtained from Charles River (Cambridge, MA).

For each cell line, s.c. tumors were established by injecting human pancreatic cells (1×10^6 PSN1 and 2.5×10^6 Panc1) in a volume of 150 μl into the right flanks of female nude (*nu/nu*) mice at 6–8 weeks of age. Each treatment group consisted of five mice. Five days after s.c. injection of tumor cells, the treatment groups received an intratumor injection of the therapeutic viruses. For AAV-FHIT, 5×10^8 infectious particles/tumor were injected. In the Ad-FHIT treatment group, animals received 2×10^{10} PFUs/tumor. The control groups received an intratumor injection with AAV-GFP (5×10^8 infectious particles/tumor) or Ad-GFP (2×10^{10} PFUs/tumor). For each cell line, a group of five animals received an intratumoral injection of 100 μl of PBS 5 days after tumor injection as control. The animals were monitored twice weekly for tumor formation up to 2 months after inoculation. Tumor volume data, obtained from measurements of tumor dimensions by using linear calipers, were plotted on a graph. At termination of the experiment, tumors were excised for histology and assessment of Fhit expression by immunocytochemical detection.

To mimic peritoneal dissemination of pancreatic cancer, 1×10^6 PSN1 cells were transplanted into the peritoneal cavity of 12 *nu/nu* mice (day 0). i.p. inoculation of PSN1 results in the formation of multiple small nodules on the mesentery and formation of tumor nodules on and in the pancreas within 4–6 days (27). For the treatment group, four mice received two sequential i.p. injections of 150 μl (2×10^{10} PFUs) of Ad-FHIT virus at days 4 and 8. A control group was treated with Ad-GFP in the same manner, and a group of four mice was left untreated. The 12 mice were observed over 28 days. When tumor development was manifest (abdominal swelling), mice were sacrificed and examined for tumors in the peritoneal cavity. All remaining animals were sacrificed 28 days after the first injection of virus. Histological sections were made from the pancreas, spleen, small intestine, and colon.

Statistical Analyses. Data are reported as means ± SE. Statistically significant differences ($P < 0.05$) between groups were detected using unpaired *t* test, paired *t* test, and nonparametric tests, such as the Wilcoxon signed rank test and the Mann-Whitney Rank Sum test, where appropriate for the data. For categorical data, we used the χ^2 test.

RESULTS

We carried out *in vitro* experiments to evaluate the effect of Fhit overexpression on pancreatic tumor cell growth. Because the inactivation of the *FHIT* gene may lead to tumor growth, replacement of the mutated tumor suppressor gene with the wild-type construct could result in restoration of the tumor suppressor activity. Therefore, we evaluated the effect of Ad- and AAV-mediated Fhit overexpression on human pancreatic cancer cell proliferation, apoptosis, and cell cycle control.

Cell Line Characteristics. The observed *in vitro* effects may well rely on the efficiency of the transgene expression vectors used and probably also depend on the functional status of *FHIT* and other genes altered in pancreatic cancer, such as KRAS and TP53. Cell lines were selected on the basis of their FHIT status or Fhit protein expression and efficiency of infection with Ad and AAV viruses.

As summarized in Table 1, the level of Fhit expression in pancreatic cancer cell lines was assessed by Western blot analysis and immunohistochemistry. Also the single-strand conformational variant analysis data for FHIT (7, 13) and the mutational status of KRAS and TP53, as reported previously (31–33), were determined. The expression of cell surface HSPG and $\alpha V\beta 5$ integrin (34) and the receptor for human fibroblast growth factor (FGFR-1; Ref. 30) was also measured. These surface molecules were identified as receptors for AAV type 2 attachment and uptake (35) and may represent an alternative route for adenovirus entry into the cell (36, 37).

AAV and Ad Infection of Pancreatic Cancer Cell Lines: Transduction Levels. To determine the efficiency of gene expression after AAV infection, quantitative analysis was performed in different human pancreatic cancer cell lines (AsPc1, HPAF, BxPc3, Panc1, Hs766T, Capan1, Capan2, MiaPaca, CFPAC, and PSN1), and the relative transduction efficiency of AAV into the cell lines was compared with the transduction level of the cervical cancer cell line HeLa, which is highly permissive for AAV infection (30). Cells were plated in triplicate at a density of 10^5 cells/well in 48-well culture plates and infected with AAV-GFP (1×10^5 viral particles/cell). GFP-expressing cells were visualized *in vitro* by confocal microscopy and by the fraction of GFP-expressing cells measured by FACS analysis. Comparable with data reported previously (30), ~70% of HeLa cells were transduced by AAV-GFP. The pancreatic cancer cell lines BxPc3, Panc1, PSN1, AsPc1, and Capan1 were also efficiently transduced. Because of their lower transduction levels for AAV, the cell lines HPAF, Hs766T, Capan2, MiaPaca, and CFPAC were excluded from additional studies.

For Ad viruses, the transduction efficiency was determined by examining the level of GFP-expressing cells in the Ad-GFP-transduced cell population by confocal microscopy and FACS analysis. The transduction efficiency is presented at the highest MOI applied for each cell line (Table 1). In additional experiments, the AAV-GFP and the Ad-GFP vector were used to monitor transduction efficiency by the viral vectors and as nonspecific transgene expression controls.

Table 1 *Cell line characteristics*[a]

	FHIT status[b]			Gene status[c]		Transduction levels		Surface marker expression		
Cell line	W-Blot	IHC	*FHIT* gene (SSCV)	*TP53*	*KRAS*	AAV	Ad	$\alpha v\beta 5$	FGF	HSPG
PANC1	Neg	Neg	Exon 7, polymorph	Mutated	Mutated	27 ± 4	98 ± 2 (50)	59 ± 6	22 ± 4	3 ± 1
PSN1	Neg	Neg	ND	Mutated	Mutated	34 ± 7	99 ± 3 (50)	64 ± 8	8 ± 2	ND
BxPc3	Neg	Neg	Exon 4, polymorph Exon 5, no amplification	Mutated	Nl	32 ± 6	47 ± 5 (100)	18 ± 4	6 ± 1	3 ± 1
AsPc1	Pos	Pos	Exon 8, polymorph	Mutated	Mutated	18 ± 5	38 ± 8 (100)	69 ± 8	6 ± 2	3 ± 1
Capan1	Pos	Pos	ND	ND	ND	19 ± 2	46 ± 5 (100)	12 ± 4	5 ± 2	6 ± 2
HeLa						71 ± 6	92 ± 4	80 ± 6	20 ± 4	5 ± 1

[a] All experiments were conducted in triplicate.
[b] W-blot, Western blot; IHC, immunocytochemistry; Neg, negative; Pos, positive; ND, not done; Nl, normal; SSCV, single-strand conformational variant analysis for FHIT (7, 13).
[c] *TP53* mutations (32, 33) and *KRAS* (27) AAV transduction, represented as mean percentage ± SD of cells expressing GFP, Ad: percentage of cells expressing GFP at highest MOI used indicated in brackets, % of cells expressing $\alpha v\beta 5$, fibroblast growth factor, or HSPG.

Downloaded from http://aacrjournals.org/cancerres/article-pdf/61/12/4827/2486769/4827.pdf by guest on 24 August 2022

AAV-FHIT Infection of Pancreatic Cancer Cell Lines: Effect on Morphology, Cell Cycle, DNA Fragmentation, and Apoptosis. At first, we evaluated the *in vitro* effect of AAV-FHIT on cell proliferation and growth. For these experiments, cells were seeded in 12-well or 24-well plates. Five days after AAV-FHIT infection, Western blot analysis showed clear Fhit expression in crude protein extracts of HeLa, Panc1, and BxPc3 cells (Fig. 1*E*). Microscopic evaluation showed apparent morphological changes such as cytoplasmic blebbing, shrunken cytoplasm, and loss of membrane integrity in AAV-FHIT-infected cells, which was not noted in mock-infected or AAV-GFP-infected cells (Fig. 1*A*). Cell counting showed a clear reduction in the number of cells with a concomitant increase in the number of dead cells after AAV-FHIT infection, which was not observed after AAV-GFP or mock infection. To exclude the possibility that preincubation with tyrphostin 1 affected cell survival, Panc1 cells were infected with AAV-GFP or AAV-FHIT with and without tyrphostin 1. Preincubation with tyrphostin 1, which leads to accelerated transcription of the transgene, increased the percentage of dead cells after AAV-FHIT transduction but did not affect mock and AAV-GFP-transduced cells (Fig. 1*C*).

As shown in Fig. 2*B*, results for individual pancreatic cancer cell lines displayed a marked increase of the proportion of dead cells after *in vitro* AAV-FHIT infection. The effect was more prominent at a higher AAV-FHIT viral load and was not seen in AAV-GFP-infected cells. The lung cancer cell line A549, which was shown previously to undergo apoptosis by Ad-FHIT overexpression (14), was included for this aspect of the study. The effect of AAV-FHIT on the cell lines AsPc1 and Capan1, which both express endogenous Fhit, was less prominent (Fig. 2*B*).

LM-PCR, performed on DNA extracts of A549 and Panc1 cells, revealed DNA ladder formation in extracts of AAV-FHIT-transduced cells, which suggests that the activation of apoptotic pathways was the underlying mechanism leading to increased cell death (Fig. 1*D*). Cell cycle analysis was performed on individual cell lines, as shown for the pancreatic cancer cell line BxPc3. Cells infected with AAV-FHIT showed a clear increase in the fraction of hypodiploid cells (sub-G_1) 5 days after AAV-FHIT infection, which was not noted with wild-type cells or AAV-GFP transduction. A simultaneous increase in the number of DNA fragments, measured by FITC labeling of single- and double-strand breaks, was also noted (Fig. 1*B*).

Fig. 2*A* summarizes the data obtained for different cell lines analyzed (Panc1, BxPc3, PSN1, A549, Capan1, and AsPc1). Five days after transduction, a significant and dose-dependent reduction of 41 and 67% in cell number was noted for AAV-FHIT-transduced cells. No difference in cell count between untreated and AAV-GFP-transduced cells was noted ($P < 0.05$ for FHIT2 *versus* Nl and $P < 0.05$ for FHIT4 *versus* Nl; Fig. 2*A*). There was a >100% increase in the number of dead cells, measured by trypan blue staining in the AAV-FHIT-transduced cell lines compared with the control groups of mock- and AAV-GFP-transduced cells (Fig. 2*A*). This was paired with a doubling of the amount of DNA strand breaks in AAV-FHIT-transduced cells, measured by FACS as exemplified for BxPc3 in Fig. 1*B* ($P < 0.05$ FHIT4 *versus* Nl, FHIT2 *versus* NL).

Ad-FHIT Effect on Cell Cycle. We performed parallel experiments with the same cell lines using an Ad vector (Ad-FHIT). Ad Fhit overexpression had the same inhibitory effect on *in vitro* cell proliferation as observed with AAV-FHIT. The Ad-FHIT virus was then used to analyze specific aspects, such as changes in cell cycle distribution, activation of proapoptotic molecules, and changes in susceptibility to external stimuli, induced by Fhit overexpression.

To study cell cycle alterations induced by Fhit overexpression, each cell line was infected with various MOIs of Ad-FHIT. Cells treated with Ad-GFP were used as controls. Cells were stained with PI and analyzed by FACS. Fig. 3 displays the changes in the subdiploid (sub-G_1), G_1, S, and G_2 fractions observed for the individual cell lines. For BxPc3, the apoptotic sub-G_1 fraction was 69% at a MOI of 50. At this MOI, ±42% of BxPc3 cells were infected by Ad-FHIT. The increase in the subdiploid fraction was paralleled with a dramatic decline in the G_1, S, and G_2 fractions of the cell cycle. As detailed in Fig. 3, similar effects were noted for PSN1 and Panc1. For AsPc1, the sub-G_1 fraction was 15% at a MOI of 50 compared with 9% in the mock and 12% in the Ad-GFP-transduced cells with ~36% of cells

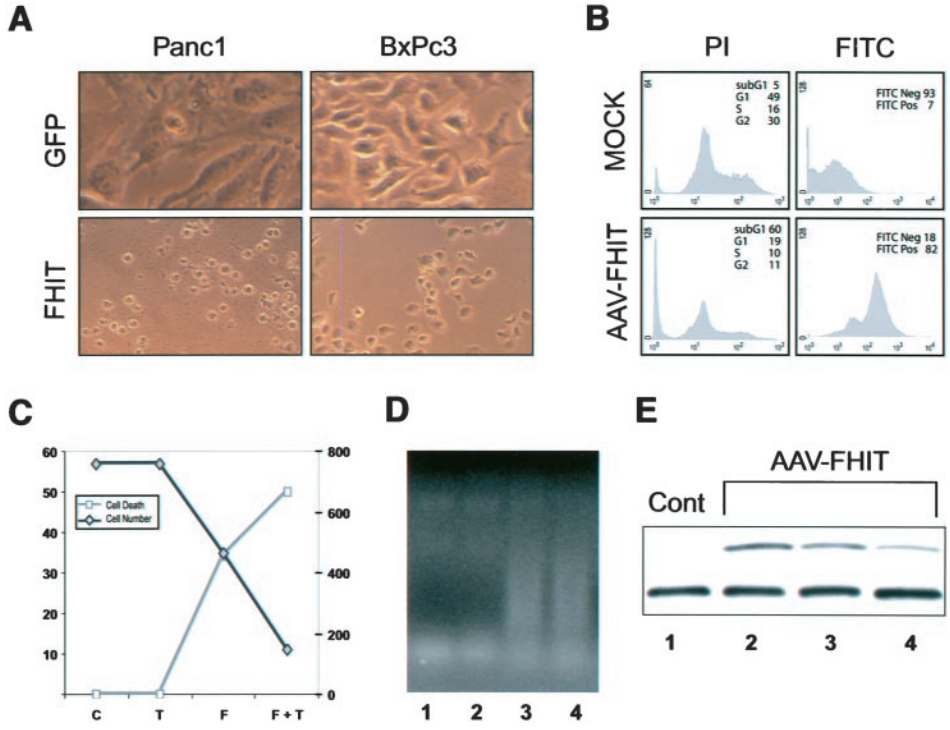

Fig. 1. AAV-FHIT infection of pancreatic cancer cell lines: effect on morphology, cell cycle, and DNA fragmentation. *A*, different morphological aspects of AAV-GFP (*GFP*)- and AAV-FHIT (*FHIT*)-infected cells. *B*, cell cycle analysis of mock- and AAV-FHIT-infected BxPc3 cells (*PI*) and the level of FITC-labeled DNA breaks in mock- and AAV-FHIT-infected BxPc3 cells (*FITC*). *C*, cell count and percentage of dead cells in AAV-GFP-infected Panc1 cells without (*C*) and with (*T*) tyrphostin preincubation and in AAV-FHIT-infected cells without (*F*) and with (*F*+*T*) tyrphostin preincubation. *D*, DNA ladder formation in AAV-FHIT-infected Panc1 (*Lane 3*) and A549 (*Lane 4*) cells compared with AAV-GFP-infected (*Lane 2*) and mock-infected (*Lane 1*) Panc1 cells. *E*, Western blot showing Fhit expression in HeLa (*Lane 2*), Panc1 (*Lane 3*), and BxPc3 (*Lane 4*) cells after AAV-FHIT infection compared with uninfected BxPc3 cells (1).

Downloaded from http://aacrjournals.org/cancerres/article-pdf/61/12/4827/2486769/4827.pdf by guest on 24 August 2022

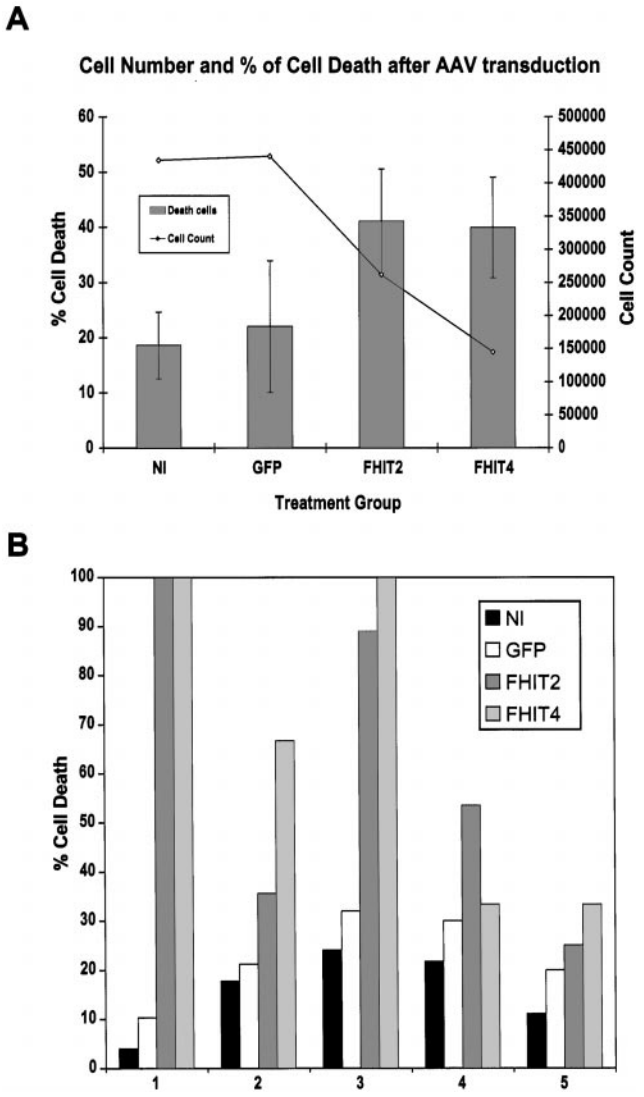

Fig. 2. AAV-FHIT infection of cancer cell lines: effect on apoptosis. *A*, results of different pancreatic cancer cell lines (Panc1, Capan1, Aspc1, and BxPc3) as well as the lung cancer cell line A549 and the cervical cancer cell line HeLa combined. Cell counts and the percentage of dead/apoptotic cells assessed by trypan blue exclusion and bromodeoxyuridine-labeled DNA strand breaks are shown; *bars*, SE. *B*, effect on individual cell lines: the percentage of dead cells in mock-infected (*NI*), AAV-GFP at 4×10^5 viral particles/cell (*GFP*) and AAV-FHIT-infected cells at two different AAV-FHIT viral loads, 2×10^5 viral particles/cell (*FHIT2*) and 4×10^5 viral particles/cell (*FHIT4*). *Columns 1*, BxPc3; *columns 2*, Panc1; *columns 3*, A549; *columns 4*, Capan1; *columns 5*, AsPc1.

infected. For Capan1, the subdiploid fraction was 14% with Ad-FHIT at an MOI of 50, compared with 15% in the mock-transduced and 12% in the Ad-GFP-transduced cells. At this MOI, 41% of Capan1 cells were infected by Ad-FHIT (Fig. 3).

Ad-FHIT Effect on Mitochondrial Apoptosis. As shown in Fig. 4, combined nuclear and mitochondrial staining of Panc1 cells infected with Ad-FHIT showed that Fhit overexpression leads to mitochondrial alteration as well as nuclear fragmentation. In healthy Panc1 cells, the dye (Mitosensor) is taken up in the mitochondria, where it forms aggregates that exhibit red fluorescence, and the blue-stained nucleus appears intact (Fig. 4*A*). In Ad-GFP-transduced cells, the GFP protein is present in the cytoplasm, and red fluorescence, indicating normal mitochondrial activity, is still present (Fig. 4*B*). In Ad-FHIT-transduced cells, the nucleus has a fragmented appearance, and because of a lack of mitochondrial membrane potential, MitoSensor remains in the cytoplasm in monomeric form, where it exhibits green fluorescence (Fig. 4*C*), indicating that the mitochondrial pathway of apoptosis is activated by Ad-FHIT.

Modulation of Mitochondrial and Cytoplasmic Apoptosis-related Proteins by Ad-FHIT. To characterize whether caspases, the major mediators of the classical apoptosis pathways, are involved in death induced by Fhit, we measured the modulation of activity of specific mitochondrial and cytoplasmic caspase-related proteins such as caspase-8, caspase-3, caspase-9, PARP, and Bid. We infected Panc1 cells with increasing MOI and monitored the proportion of transduced cells by confocal microscopy and FACS analysis. To exclude virus-specific effects, we compared cell lysates from cells infected with Ad-GFP and Ad-GFP-FHIT at the same MOI. As shown in Fig. 5, the morphology of Ad-FHIT-infected cells displayed typical apoptotic changes, such as blebbing and shrinkage of cytoplasm, which was not seen in Ad-GFP-transduced or uninfected cells (Fig. 5). At MOI of 10 and 50, strong expression of Fhit is seen in Ad-GFP-FHIT-infected Panc1 cells. As further shown in Fig. 5, a distinct activation pattern can be discerned by comparison of Ad-GFP-FHIT- and Ad-GFP-infected Panc1 cells. Initiators caspase-8 and caspase-9 were activated in Ad-GFP-FHIT-transduced cells. Western blot analysis showed that the M_r 55,000 precursor form of caspase-8 was cleaved to the active M_r 18,000 fragment. Caspase-9, which is activated after release of cytochrome *c* from mitochondria, was also activated in Ad-GFP-FHIT-infected cells. The M_r 32,000 precursor of

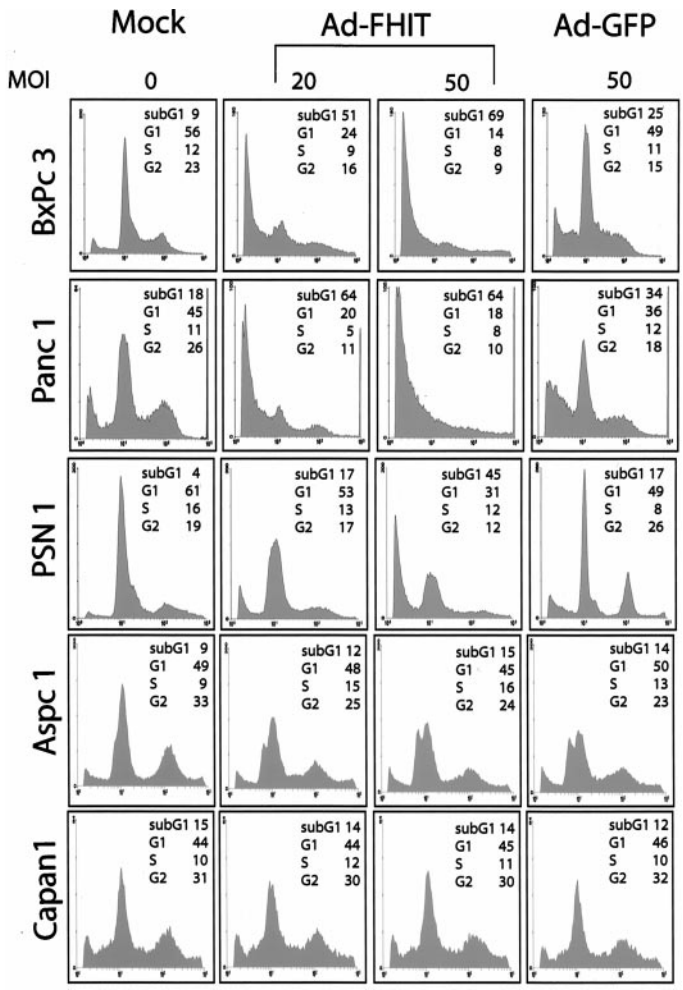

Fig. 3. Ad-FHIT effect on cell cycle. The cell cycle distribution for cell lines BxPc3, Panc1, PSN1, AsPc1, and Capan1 (sub-G_1, G_1, S, and G_2) at two MOI of Ad-FHIT, compared with mock- and Ad-GFP-infected cells. Cells with subdiploid DNA content (sub-G_1) are considered apoptotic.

Downloaded from http://aacrjournals.org/cancerres/article-pdf/61/12/4827/2486769/4827.pdf by guest on 24 August 2022

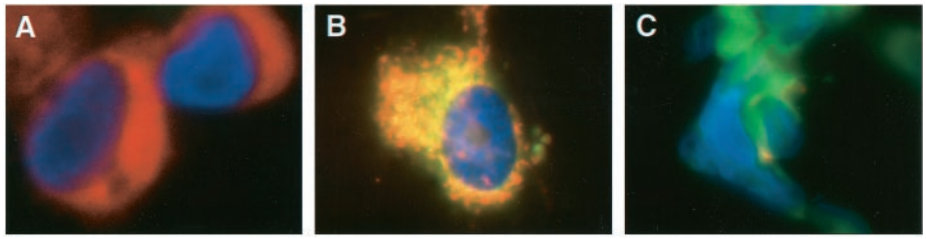

Fig. 4. Ad-FHIT effect on mitochondrial membrane potential. *A*, in untreated Panc1 cells, the dye (Mitosensor) is taken up in the mitochondria, where it forms aggregates that exhibit red fluorescence and the blue-stained nucleus appears intact. *B*, Ad-GFP infected cells show green staining indicating GFP transgene expression as well as red fluorescence in the mitochondria, which indicates normal mitochondrial activity. *C*, in Ad-FHIT-infected cells, the nucleus has a fragmented appearance and because of the lack of mitochondrial membrane potential, MitoSensor remains in the cytoplasm in monomer form, where it exhibits green fluorescence, indicating that the mitochondrial pathway of apoptosis is activated.

the effector caspase-3 was cleaved to the M_r 19,000 fragment. As further shown, cellular proteins such as PARP, known to be activated downstream by caspase-3, were cleaved. Also Bid, known to be activated by caspase-8 and caspase-3, was cleaved in Ad-GFP-FHIT-infected cells. In contrast, these proapoptotic proteins were not activated in native or Ad-GFP-infected cells.

Effect of Proapoptotic Exogenous Signals on Ad-FHIT-infected Cells. Because proapoptotic extracellular signals, such as TNF-α and Fas ligand, function through activation of caspase pathways, we examined whether Ad-FHIT-infected PSN1 and Panc1 cells were more susceptible to proapoptotic signals, such as cytokine stimulation by TNF-α, FAS ligand, and IFN-γ. PSN1 and Panc1 cells were infected with Ad-GFP-FHIT at the MOI known to induce apoptosis in ~20% of the cell population. Ad-GFP infection at the same MOI and untreated cells were used as controls.

Because the initial *in vitro* data (Fig. 3) showed a higher susceptibility of Panc1 to FHIT-induced apoptosis compared with PSN1 (Panc1, sub-G_1 of 64% at MOI 20 compared with PSN1, sub-G_1 of 17% at MOI 20), we conducted the external stimulation assays at different MOI for the two cell lines (MOI 20 for PSN1 *versus* MOI 10 for Panc1) to allow for comparable levels of apoptotic fractions with Ad-GFP-FHIT. As expected, uninfected Panc1 and PSN1 cells, shown previously to be resistant to TNF-α and Fas antibody, showed only a marginal response to IFN-γ, Fas antibody, and TNF stimulation.

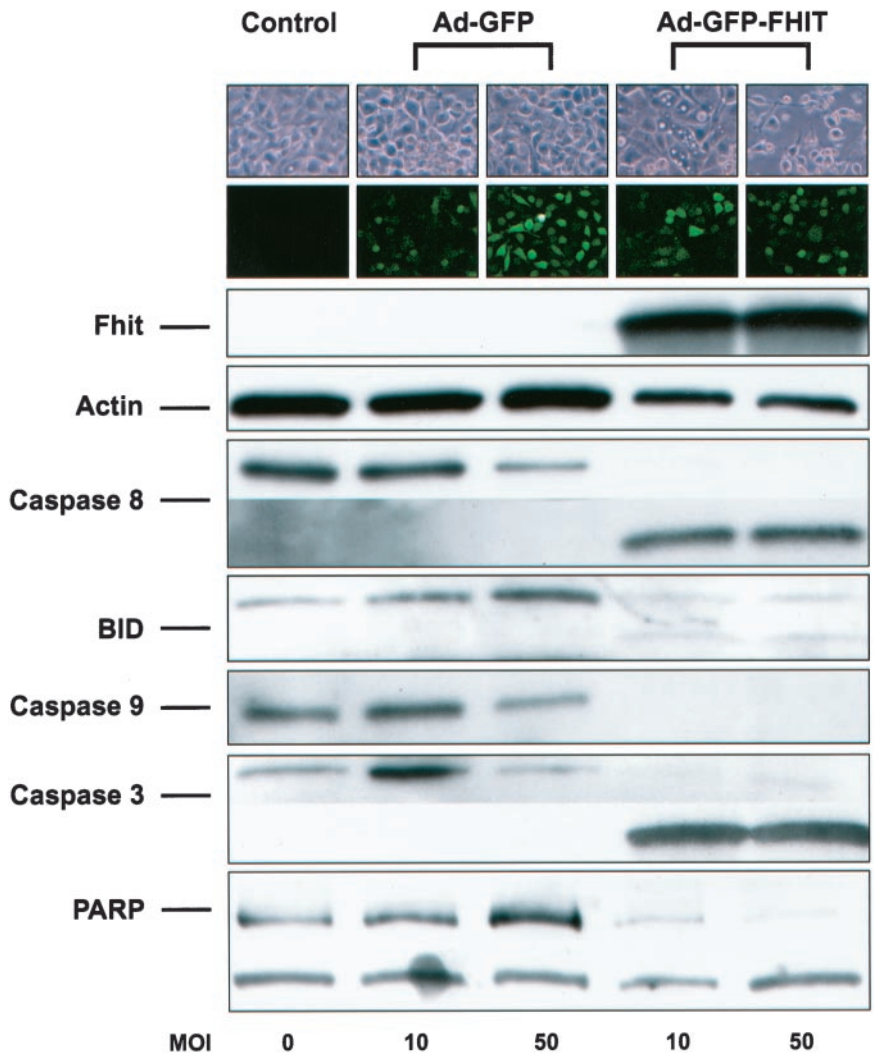

Fig. 5. Modulation of mitochondrial and cytoplasmic apoptosis-related proteins by Ad-FHIT. Panc1 cells (*Control*) are compared with Ad-GFP-infected (*Ad-GFP*) and Ad-GFP-FHIT-infected (*Ad-GFP-FHIT*) cells. Cell morphology (*first row*) and level of GFP expression (*second row*) are displayed for MOI of 10 and 50. Western blot shows equal amounts of actin, with Fhit expression only in cell lysates from Ad-GFP-FHIT-infected cells (*Fhit*). The M_r 55,000 precursor form of caspase-8 was cleaved to the active M_r 18,000 fragment in Ad-GFP-FHIT-infected cells (*Caspase 8*). The M_r 32,000 precursor of the effector caspase-3 is cleaved to the M_r 19,000 fragment (*Caspase 3*). The caspase-9 precursor is reduced in Ad-GFP-FHIT-infected cells, indicating activation (*Caspase 9*). The M_r 23,000 Bid precursor is cleaved in Ad-GFP-FHIT-infected cells (*BID*). Activation of the M_r 116,000 native PARP yields a M_r 85,000 fragment (*PARP*).

Downloaded from http://aacrjournals.org/cancerres/article-pdf/61/12/4827/2486769/4827.pdf by guest on 24 August 2022

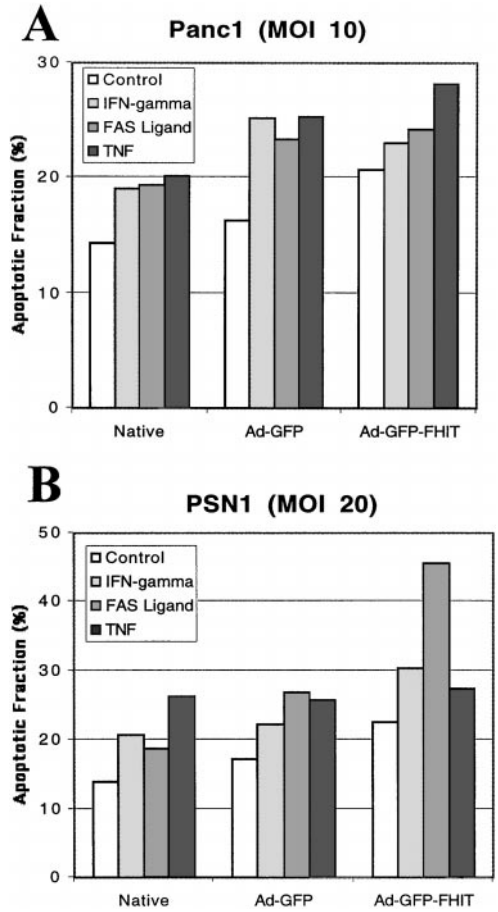

Fig. 6. Effect of proapoptotic exogenous signals on Ad-FHIT-infected cells. Results for two cell lines, Panc1 (*A*) and PSN1 (*B*) are shown. Panc1 cells were infected with MOI 10, and PSN1 cells were infected with MOI of 20. Untreated PSN1 and Panc1 cells *(Native)* or infected with Ad-GFP *(Ad-GFP)* or Ad-GFP-FHIT *(Ad-GFP-FHIT)*. On the *Y axis*, the sub-G_1 fraction under four different conditions is presented: unstimulated (*Control*) incubation with IFN-γ (*IFN-gamma*), FAS antibody (*FAS Ligand*), or TNF-α (*TNF*).

Although Fhit overexpression augmented the effect of the three cytokine stimuli, this effect was only marginal in Panc1 cells. In contrast, Ad-GFP-FHIT-transduced PSN1 cells showed a marked increase in susceptibility to Fas antibody stimulation, suggesting sensitization to Fas through Fhit expression in PSN1 cells (Fig. 6).

***In Vivo* Reduction of Tumor Growth with AAV-FHIT and Ad-FHIT.** Both viral vectors were used to evaluate the *in vivo* effect of viral *FHIT* gene transfer on tumor growth in xenografts of poorly differentiated pancreatic cancer cell lines (PSN1 and Panc1) in nude mice. When the tumors reached 5–10 mm in diameter, the tumors were directly injected with Ad-FHIT or AAV-FHIT virus. In four separate *in vivo* experiments, growth was significantly suppressed in tumors of mice treated with Ad-FHIT or AAV-FHIT. The suppression of tumor growth by Fhit was observed for each of the two cell lines used in this experiment (Panc1 and PSN1, $P < 0.05$ Ad-FHIT *versus* Ad-GFP, $P < 0.05$ AAV-FHIT *versus* AAV-GFP). In contrast, we did not observe significant differences in tumor growth between tumors treated with Ad-GFP or AAV-GFP and untreated tumors (Fig. 7). After sacrificing the animals, sections of tumors were stained for human Fhit protein by immunohistochemistry. Only tumor sections of mice treated with the therapeutic FHIT vectors showed Fhit expression, which confirms efficient delivery of the transgene at the cellular level. For most sections, the Fhit expression pattern was not uniform, which may be attributable to tumor clones that escaped the initial viral infection or selective growth advantage of Fhit-negative clones, as suggested previously (Refs. 38 and 39; Fig. 7, *B* and *C*).

We used a model of i.p. tumor dissemination to further evaluate the feasibility of *in vivo* Ad FHIT delivery. i.p. injection of PSN1 cells in nude mice leads to the development of tumors in the pancreas and along the mesentery (Fig. 8, *A*, *B*, and *D*), a pattern that closely resembles metastatic spread of human pancreatic cancer (27). Because previous studies have shown the development of intrapancreatic and peritoneal metastasis within 8 days of i.p. injection of a small tumor burden (1×10^5 PSN1 cells) in nude mice (40), a drastic impact on survival was expected with this study set-up. Three groups of mice received an i.p. injection of PSN1 cells. Four and 8 days after tumor cell injection, one group of mice received i.p. injections of Ad-FHIT. The control group received two i.p. injections of Ad-GFP, and one group was left untreated. All mice developed metastatic tumor growth

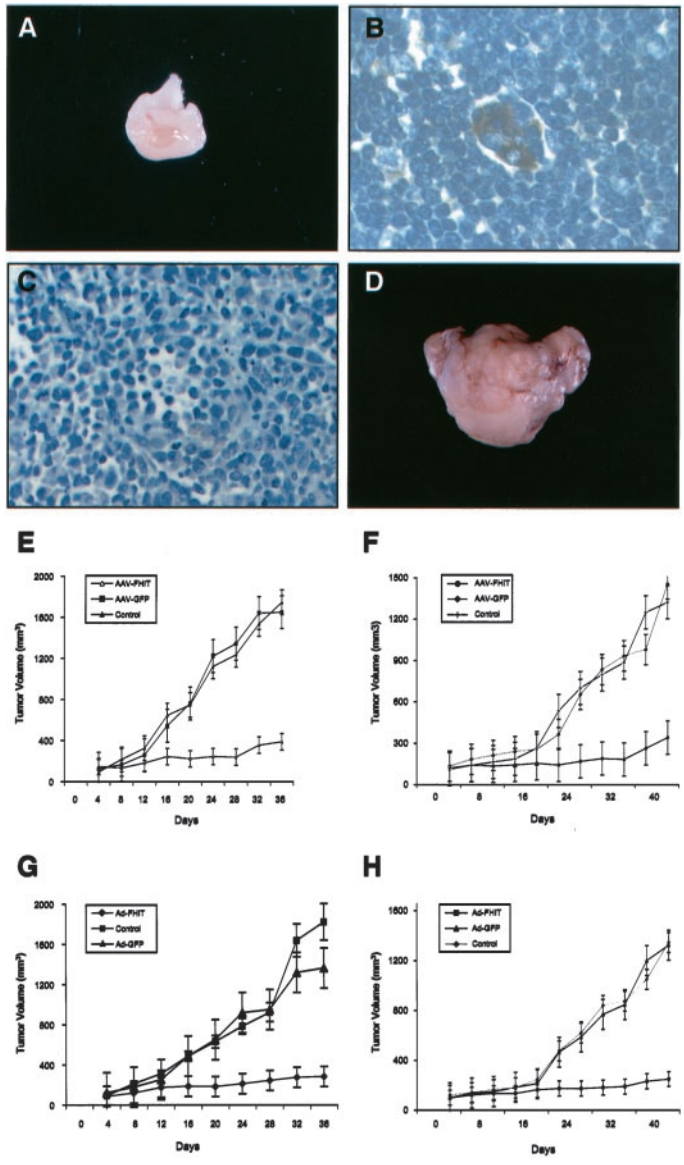

Fig. 7. Infection of s.c. tumors. Tumor phenotype of Ad-FHIT-treated (*A*) and Ad-GFP-treated (*D*) PSN1 tumors resected 30 days after s.c. tumor growth. Immunohistochemistry of tumor sections shows areas of Fhit expression in Ad-FHIT-infected tumors (*B*) with no Fhit expression in Ad-GFP-infected tumors (*C*). *In vivo* growth curves of parental (*Control*), AAV-GFP- and AAV-FHIT-infected s.c. tumors of PSN1 (*E*) and Panc1 (*F*) are shown. *In vivo* growth curves of parental (*Control*), Ad-GFP- and Ad-FHIT-infected s.c. tumors of PSN1 (*G*) and Panc1 (*H*) are shown. The data represent average tumor volume with SD for each group ($n = 5$). *Bars*, SE.

Downloaded from http://aacrjournals.org/cancerres/article-pdf/61/12/4827/2486769/4827.pdf by guest on 24 August 2022

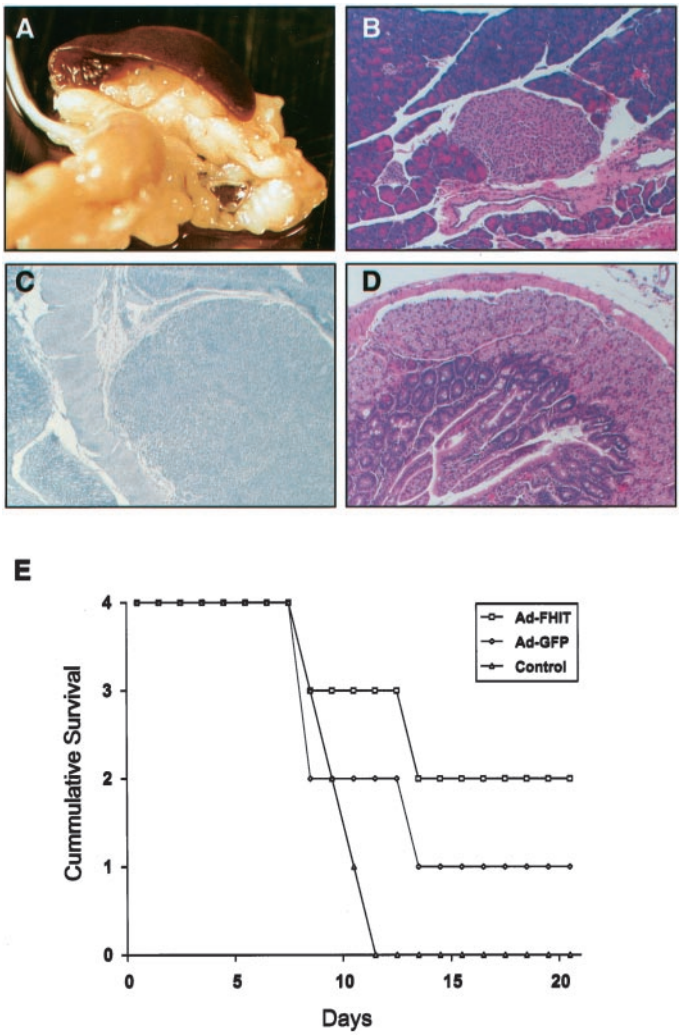

Fig. 8. Infection of i.p. tumors. Macroscopic and histological aspects of metastatic tumor formation. i.p. injection of PSN1 cells results in an extensive tumor spread to the mesentery as well as a significant tumor burden between the stomach and the spleen, corresponding to the pancreatic region (*A*). Histology sections show intrapancreatic tumor invasion (*B*) and subserosal invasion of the intestinal wall (*D*). Immunohistochemical staining of tumors of Ad-FHIT-infected animals shows absence of detectable Fhit protein (*C*). *E*, survival curve after i.p. injection of PSN1. Each group of animals received an i.p. injection of PSN1 cells. One group of animals ($n = 4$) received an i.p. injection of Ad-GFP; one group received an i.p. injection of Ad-FHIT; and one group of animals was left untreated (*Control*). A second treatment was performed on day 8. Survival of each group is shown starting from the second treatment (day 8).

(Fig. 8, *A*, *B*, and *D*), but in the Ad-FHIT treatment group, two mice survived at 20 days after the last viral dose compared with only one animal in the Ad-GFP treatment group. All of the animals left untreated after tumor injection died by day 17 (Fig. 8*E*). Immunohistochemistry failed to detect Fhit expression in tumor lesions of Ad-FHIT-treated animals (Fig. 8*C*).

In comparing the number of animals that survived on day 28, there was only a marginal difference between the Ad-FHIT treatment group and the two control groups (Ad-GFP and untreated). We compared survival in the Ad-FHIT-treated group *versus* the control group ($P = 0.10$, χ^2) and the Ad-FHIT-treated group *versus* the two control groups (untreated and Ad-GFP combined; $P = 0.16$, χ^2). There was no statistically significant difference between the untreated group and the Ad-GFP-treated group ($P = 0.28$). When we looked at the difference in survival, counted in days, among the three groups, there was a statistically significant increase in survival in the Ad-FHIT-treated group (median of 25 days) compared with both control groups ($P < 0.05$ Ad-FHIT *versus* Control and $P < 0.05$ Ad-FHIT *versus* Control + Ad-GFP, Mann-Whitney Rank Sum Test). In contrast, there was no significant difference in survival between the Ad-GFP-treated animals (median of 18.5 days) and the group of animals left untreated (median of 16.5 days).

DISCUSSION

Given the aggressive biological nature of pancreatic cancer and the urgent need for new therapeutic strategies, we evaluated an approach that targets the disease at the molecular level by viral transfer of the human *FHIT* gene into human pancreatic cancer cells. We have shown that Fhit overexpression mediated by an Ad or AAV vector induces apoptosis in pancreatic cancer cells lacking endogenous Fhit. Virus-mediated Fhit overexpression leads to activation of the two main proapoptotic caspase cascades, mitochondrial-mediated caspase-3 activation through caspase-9 (intrinsic pathway) and the death receptor-induced caspase-3 activation by caspase-8 (extrinsic pathway). Also, an enhanced sensitivity to external proapoptotic stimuli (FAS) in cells overexpressing Fhit was noted. Intratumoral injection of Ad or adenoassociated FHIT vectors led to a significant *in vivo* suppression of tumor growth in nude mice, and i.p. injection of Ad-FHIT prolonged survival in a mouse peritoneal dissemination model of human pancreatic cancer.

The Use of FHIT as a Therapeutic Tumor Suppressor. After the first description of alterations in the *FHIT* gene locus in the renal carcinoma-associated t(3;8) breakpoint and in digestive tract tumors (41), an extensive amount of data supported the role of *FHIT* as a tumor suppressor gene in human cancer (reviewed in Ref. 12). Loss of Fhit expression has been studied in most gastrointestinal tumors, and two independent studies confirmed loss of FHIT in ~66% of pancreatic cancer cell lines and primary pancreatic cancers (7, 13). In both studies, the lack of Fhit protein expression correlated with absence or alteration of FHIT mRNA and was associated with *FHIT* gene anomalies. In these studies, homozygous deletion of the *FHIT* exon 5 was the most frequent gene alteration found. Our results show that Ad FHIT, shown previously to induce apoptosis in human lung (14) and esophageal (15) cancer, also induces apoptosis and reduces tumor growth in pancreatic cancer. Furthermore, we showed that AAV-FHIT leads to the same *in vitro* proapoptotic and *in vivo* tumor-reducing effect. This extends the role of *FHIT* as a tumor suppressor gene to pancreatic cancer.

AAV-FHIT- and Ad-FHIT-induced Apoptosis Depends on *FHIT* Status. The *FHIT*, *TP53*, and *KRAS* status of the cell lines selected for this study are listed in Table 1. Three of the cell lines tested (PSN1, Panc1, and BxPc3) lacked Fhit expression, whereas Capan1 and AsPc1 expressed Fhit. DNA analysis also showed that exon 5, the first protein-coding exon, was missing in BxPc3[5] with no detectable wild-type *FHIT* mRNA present in these cell lines. Reexpression of Fhit in cell lines lacking Fhit, such as PSN1, Panc1, and BxPc3, leads to apoptosis. In contrast, pancreatic cancer cell lines that express Fhit, such as Capan1 and AsPc1, did not show a clear increase of the apoptotic fraction. We therefore concluded that the apoptotic effect induced by Fhit in pancreatic cancer is primarily dependent on the Fhit status and is p53 independent. Interestingly, all pancreatic cell lines tested had a mutated *p53* and K-*ras* gene, which confirms the observation that Fhit mediates apoptosis independently of other tumor suppressor genes, such as *p53* (16). Similarly, Ji *et al.* (14) observed Ad-FHIT-induced apoptosis in human lung cancer cells with loss of Fhit expression, but the head and neck cancer cell line 22B, which expresses Fhit, was not affected. Also in this study, the susceptibility

[5] T. Druck, data not shown.

Downloaded from http://aacrjournals.org/cancerres/article-pdf/61/12/4827/2486769/4827.pdf by guest on 24 August 2022

to Fhit was independent of the p53 status of the cell lines (14). Using stable transfectants, Werner *et al.* (39) observed that a moderate elevation of Fhit expression in renal cancer cells with low-level expression of endogenous Fhit was sufficient for the induction of tumor suppression *in vivo*. This is in agreement with the observation reported previously of apoptosis in one of the esophageal cancer cell lines expressing Fhit (15) and indicates that Fhit-induced apoptosis is not limited to cancer cells completely lacking Fhit. Similar to observations with other tumor suppressor genes (such as *p53*), the previously reported failure to detect any tumor suppressor effect of Fhit in specific cancer cell lines that either lack or express residual low levels of Fhit may reflect a disruption in the effector molecules downstream of the Fhit pathway (42, 43). Also, previous studies showed that Fhit is not toxic to normal cells; Fhit did not affect growth of nontumorigenic epithelial cells (14, 15) such as transformed human embryonic kidney cells (38), normal human bronchial epithelial cells, which express both normal FHIT transcripts and Fhit protein (14), or normal small airway bronchial epithelial cells infected with Ad-FHIT (15).

Ad-FHIT Overexpression Activates Mitochondrial and Cytoplasmic Proapoptotic Pathways. Our results indicate that reintroduction of FHIT may restore the proapoptotic potential of some cancer cells. It is a well-established concept that impaired apoptosis signaling is common in cancer cells and that it may play an important role in tumor initiation and progression (43–46). Mutations in apoptosis-regulatory genes may lead to a disruption of endogenous induction pathways, such as those involving p53, death receptors, or apical caspase activation, which leads to resistance of cancer cells to apoptosis. This is especially deleterious because it not only enhances the spontaneous growth of tumors but also renders them resistant to host defense mechanisms, as well as various forms of cancer therapy (42). We showed that Fhit overexpression mediated by an Ad or AAV vector leads to apoptosis in pancreatic cancer cells lacking endogenous Fhit, with typical characteristics such as loss of mitochondrial membrane potential as a sign of mitochondrial apoptosis and a clear increase in DNA fragmentation, paired with an increase in the proportion of hypodiploid cells. Fhit overexpression leads to activation of the extrinsic caspase pathway with activation of the initiator caspase-8 and its downstream effector, caspase-3, and the nuclear protein PARP. The concomitant cleavage of Bid confirms that the intrinsic mitochondrial pathway of apoptosis is also activated, which explains the observation of loss of mitochondrial membrane potential after Fhit overexpression. Activation of Bid leads to subsequent translocation of Bid into the mitochondria, which results in the observed caspase-9-dependent activation of the effector caspase-3 (43). We showed previously that treatment with either a potent broad-spectrum caspase inhibitor, z-Val-Ala-Asp, or an inhibitor of caspase 3-like caspases, Z-Asp-Glu-Val-Asp-FHK (Z-DEVD-FHK), protected from Ad-FHIT-induced death (15). The observed activation pattern of both pathways induced by Fhit expression is in agreement with the growing evidence of the presence of cross-talk between the extrinsic and intrinsic caspase pathways.

Ad-FHIT Enhanced Susceptibility to Proapoptotic Exogenous Signals May Be Cell Line Specific. Under most instances, trimerization of the death receptor Fas leads to direct activation of caspase-3 by caspase-8. However, it has been shown that the mitochondria-mediated caspase-9 activation pathway amplifies Fas signaling through caspase-8-mediated cleavage of Bid and translocation of Bid into the mitochondria (47). This could account for the difference in Panc1 and PSN1 in susceptibility to Fas ligand after Fhit overexpression; Ad-FHIT-transduced PSN1 cells showed a marked increase in susceptibility to Fas antibody-stimulated apoptosis, whereas Panc1 cells were not sensitized to Fas through Fhit expression. In some cells, the interaction of the Fas receptor with the Fas ligand can lead to a rapid proteolytic activation of caspases through recruitment of caspase-8 into the receptor complex (42, 48). Caspase-8 is known to cleave Bid (42). Many pancreatic cancer cell lines are known to be resistant to Fas-induced apoptosis, and cell line-specific differences in receptor status, as well as in the effector pathway, may account for different responsiveness of cell lines (48, 49).

AAV-FHIT and Ad-FHIT Reduces Tumor Growth and Prolongs Survival. We observed *in vivo* reduction of tumor growth with the highly tumorigenic cell lines PSN1 and Panc1 using both viral vectors. The magnitude of tumor growth suppression was similar to prior studies in which Ad FHIT vectors induced reduction of tumor growth in lung and esophageal cancer (14, 15). In contrast, some of the previous *in vitro* and *in vivo* experiments using tumor cell lines with Fhit-expressing plasmids showed variable results (38, 39). Selection pressure (42, 43), disruption of downstream pathways (42, 43), as well as the recently described compensatory mechanisms of caspase expression (48, 50) could account for some of the observed differences between individual cell lines in their susceptibility to Fhit. Furthermore, the observation that Ad-FHIT resulted in a survival benefit of mice with disseminated pancreatic tumor growth is encouraging in view of possible clinical *FHIT* gene transfer applications (28).

The *in vitro* proapoptotic effect and the *in vivo* tumor suppressor effect observed with AAV-FHIT indicate that AAV deserves further exploration as a possible vector for gene delivery in human pancreatic cancer. AAV has been studied in other fields, but its potential in pancreatic cancer has not been fully explored (29). The lower *in vitro* transduction levels observed with AAV may be caused by the need of second-strand DNA synthesis, which can be enhanced with specific agents. AAV is also not immunogenic, allows long-term expression, and is not pathogenic in humans, according to our present knowledge. Current human trials in cystic fibrosis patients receiving AAV-CFTR vectors to the upper airway and ongoing trials with i.m. or i.v. rAAV-FIX vectors for hemophilia will yield additional safety information (reviewed in Ref. 22). Clinical advances involving gene therapy will probably require cooperation with more established treatments, such as chemotherapy, radiotherapy, and immunotherapy, to show efficacy (51). Interestingly, *in vivo* gene delivery of recombinant AAV virus can be dramatically enhanced by radiation and a variety of agents, including cisplatin (52, 53), a cytostatic agent currently used in combination with radiotherapy for the treatment of pancreatic cancer (54).

The demonstration that virus-mediated Fhit overexpression reduces cell growth and induces apoptosis in human pancreatic cancer expands understanding of *FHIT* as a tumor suppressor gene and its role as a possible interventional target in this malignancy. Although limited to preclinical studies using *in vitro* and murine *in vivo* models, these initial results are encouraging. Given the devastating prognosis and lack of viable therapeutic options, pancreatic cancer may represent an opportunity in which *FHIT* gene therapy could ultimately show a clinical benefit.

REFERENCES

1. Landis, S. H., Murray, T., Bolden, S., and Wingo, P. A. Cancer statistics, 1999 [see comments]. CA Cancer J. Clin., *49:* 8–31, 1999.
2. Warshaw, A. L., and Fernandez-del Castillo, C. Pancreatic carcinoma. N. Engl. J. Med., *326:* 455–465, 1992.
3. Yeo, C. J., Cameron, J. L., Lillemoe, K. D., Sitzmann, J. V., Hruban, R. H., Goodman, S. N., Dooley, W. C., Coleman, J., and Pitt, H. A. Pancreaticoduodenectomy for cancer of the head of the pancreas. 201 patients. Ann. Surg., *221:* 721–731; discussion, 731–733, 1995.
4. Kalthoff, H., Schmiegel, W., Roeder, C., Kasche, D., Schmidt, A., Lauer, G., Thiele, H. G., Honold, G., Pantel, K., Riethmuller, G., *et al.* p53 and K-RAS alterations in pancreatic epithelial cell lesions. Oncogene, *8:* 289–298, 1993.
5. Redston, M. S., Caldas, C., Seymour, A. B., Hruban, R. H., da Costa, L., Yeo, C. J., and Kern, SE p53 mutations in pancreatic carcinoma and evidence of common

Downloaded from http://aacrjournals.org/cancerres/article-pdf/61/12/4827/2486769/4827.pdf by guest on 24 August 2022

involvement of homocopolymer tracts in DNA microdeletions. Cancer Res., *54:* 3025–3033, 1994.
6. Chen, Z. H., Zhang, H., and Savarese, T. M. Gene deletion chemoselectivity: codeletion of the genes for p16(INK4), methylthioadenosine phosphorylase, and the α- and β-IFNs in human pancreatic cell carcinoma lines and its implications for chemotherapy. Cancer Res., *56:* 1083–1090, 1996.
7. Sorio, C., Baron, A., Orlandini, S., Zamboni, G., Pederzoli, P., Huebner, K., and Scarpa, A. The *FHIT* gene is expressed in pancreatic ductular cells and is altered in pancreatic cancers. Cancer Res., *59:* 1308–1314, 1999.
8. Hwang, R. F., Gordon, E. M., Anderson, W. F., and Parekh, D. Gene therapy for primary and metastatic pancreatic cancer with i.p. retroviral vector bearing the wild-type *p53* gene. Surgery, *124:* 143–150; discussion, 150–151, 1998.
9. Jaffee, E. M., Abrams, R., Cameron, J., Donehower, R., Duerr, M., Gossett, J., Greten, T. F., Grochow, L., Hruban, R., Kern, S., Lillemoe, K. D., O'Reilly, S., Pardoll, D., Pitt, H. A., Sauter, P., Weber, C., and Yeo, C. A Phase I clinical trial of lethally irradiated allogeneic pancreatic tumor cells transfected with the GM-CSF gene for the treatment of pancreatic adenocarcinoma. Hum. Gene Ther., *9:* 1951–1971, 1998.
10. Joshi, U. S., Dergham, S. T., Chen, Y. Q., Dugan, M. C., Crissman, J. D., Vaitkevicius, V. K., and Sarkar, F. H. Inhibition of pancreatic tumor cell growth in culture by p21WAF1 recombinant adenovirus. Pancreas, *16:* 107–113, 1998.
11. Kimura, M., Tagawa, M., Takenaga, K., Yamaguchi, T., Saisho, H., Nakagawara, A., and Sakiyama, S. Inability to induce the alteration of tumorigenicity and chemosensitivity of p53-null human pancreatic carcinoma cells after the transduction of wild-type *p53* gene. Anticancer Res., *17:* 879–883, 1997.
12. Huebner, K., Garrison, P. N., Barnes, L. D., and Croce, C. M. The role of the *FHIT/FRA3B* locus in cancer. Annu. Rev. Genet., *32:* 7–31, 1998.
13. Simon, B., Bartsch, D., Barth, P., Prasnikar, N., Munch, K., Blum, A., Arnold, R., and Goke, B. Frequent abnormalities of the putative tumor suppressor gene *FHIT* at 3p14.2 in pancreatic carcinoma cell lines. Cancer Res., *58:* 1583–1587, 1998.
14. Ji, L., Fang, B., Yen, N., Fong, K., Minna, J. D., and Roth, J. A. Induction of apoptosis and inhibition of tumorigenicity and tumor growth by adenovirus vector-mediated fragile histidine triad (*FHIT*) gene overexpression. Cancer Res., *59:* 3333–3339, 1999.
15. Ishii, H., Dumon, K. R., Vecchione, A., Trappaso, F., Mimori, K., Alder, H., Mori, M., Sozzi, G., Baffa, R., Huebner, K., and Croce, C. M. Effect of adenoviral transduction of FHIT into esophageal cancer cells. Cancer Res., *G1:* 1578–1584, 2001.
16. Sard, L., Accornero, P., Tornielli, S., Delia, D., Bunone, G., Campiglio, M., Colombo, M. P., Gramegna, M., Croce, C. M., Pierotti, M. A., and Sozzi, G. The tumor-suppressor gene *FHIT* is involved in the regulation of apoptosis and in cell cycle control. Proc. Natl. Acad. Sci. USA, *96:* 8489–8492, 1999.
17. Herman, J. R., Adler, H. L., Aguilar-Cordova, E., Rojas-Martinez, A., Woo, S., Timme, T. L., Wheeler, T. M., Thompson, T. C., and Scardino, P. T. *In situ* gene therapy for adenocarcinoma of the prostate: a Phase I clinical trial. Hum. Gene Ther., *10:* 1239–1249, 1999.
18. Harvey, B. G., Leopold, P. L., Hackett, N. R., Grasso, T. M., Williams, P. M., Tucker, A. L., Kaner, R. J., Ferris, B., Gonda, I., Sweeney, T. D., Ramalingam, R., Kovesdi, I., Shak, S., and Crystal, R. G. Airway epithelial CFTR mRNA expression in cystic fibrosis patients after repetitive administration of a recombinant adenovirus [see comments]. J. Clin. Investig., *104:* 1245–1255, 1999.
19. Brody, S. L., Metzger, M., Danel, C., Rosenfeld, M. A., and Crystal, R. G. Acute responses of non-human primates to airway delivery of an adenovirus vector containing the human cystic fibrosis transmembrane conductance regulator cDNA. Hum. Gene Ther., *5:* 821–836, 1994.
20. During, M. J., Symes, C. W., Lawlor, P. A., Lin, J., Dunning, J., Fitzsimons, H. L., Poulsen, D., Leone, P., Xu, R., Dicker, B. L., Lipski, J., and Young, D. An oral vaccine against NMDAR1 with efficacy in experimental stroke and epilepsy [see comments]. Science (Wash. DC), *287:* 1453–1460, 2000.
21. During, M. J., Xu, R., Young, D., Kaplitt, M. G., Sherwin, R. S., and Leone, P. Peroral gene therapy of lactose intolerance using an adeno-associated virus vector [see comments]. Nat. Med., *4:* 1131–1135, 1998.
22. Monahan, P. E., and Samulski, R. J. AAV vectors: is clinical success on the horizon? Gene Ther., *7:* 24–30, 2000.
23. Lipkowitz, M. S., Hanss, B., Tulchin, N., Wilson, P. D., Langer, J. C., Ross, M. D., Kurtzman, G. J., Klotman, P. E., and Klotman, M. E. Transduction of renal cells *in vitro* and *in vivo* by adeno-associated virus gene therapy vectors. J. Am. Soc. Nephrol., *10:* 1908–1915, 1999.
24. Xiao, X., Li, J., and Samulski, R. J. Efficient long-term gene transfer into muscle tissue of immunocompetent mice by adeno-associated virus vector. J. Virol., *70:* 8098–8108, 1996.
25. Fisher, K. J., Jooss, K., Alston, J., Yang, Y., Haecker, S. E., High, K., Pathak, R., Raper, S. E., and Wilson, J. M. Recombinant adeno-associated virus for muscle directed gene therapy. Nat. Med., *3:* 306–312, 1997.
26. Clark, K. R., Sferra, T. J., and Johnson, P. R. Recombinant adeno-associated viral vectors mediate long-term transgene expression in muscle. Hum. Gene Ther., *8:* 659–669, 1997.
27. Aoki, K., Yoshida, T., Matsumoto, N., Ide, H., Hosokawa, K., Sugimura, T., and Terada, M. Gene therapy for peritoneal dissemination of pancreatic cancer by liposome-mediated transfer of herpes simplex virus thymidine kinase gene. Hum. Gene Ther., *8:* 1105–1113, 1997.
28. Bouvet, M., Bold, R. J., Lee, J., Evans, D. B., Abbruzzese, J. L., Chiao, P. J., McConkey, D. J., Chandra, J., Chada, S., Fang, B., and Roth, J. A. Adenovirus-mediated wild-type *p53* tumor suppressor gene therapy induces apoptosis and suppresses growth of human pancreatic cancer [see comments]. Ann. Surg. Oncol., *5:* 681–688, 1998.
29. Grimm, D., Kern, A., Rittner, K., and Kleinschmidt, J. A. Novel tools for production and purification of recombinant adenoassociated virus vectors. Hum. Gene Ther., *9:* 2745–2760, 1998.
30. Qing, K., Mah, C., Hansen, J., Zhou, S., Dwarki, V., and Srivastava, A. Human fibroblast growth factor receptor 1 is a co-receptor for infection by adeno-associated virus 2 [see comments]. Nat. Med., *5:* 71–77, 1999.
31. Aoki, K., Yoshida, T., Matsumoto, N., Ide, H., Sugimura, T., and Terada, M. Suppression of Ki-ras p21 levels leading to growth inhibition of pancreatic cancer cell lines with Ki-ras mutation but not those without Ki-ras mutation. Mol. Carcinog., *20:* 251–258, 1997.
32. Kohl, N. E., Wilson, F. R., Mosser, S. D., Giuliani, E., de Solms, S. J., Conner, M. W., Anthony, N. J., Holtz, W. J., Gomez, R. P., Lee, T. J., *et al.* Protein farnesyltransferase inhibitors block the growth of ras- dependent tumors in nude mice. Proc. Natl. Acad. Sci. USA, *91:* 9141–9145, 1994.
33. Furuwatari, C., Yagi, A., Yamagami, O., Ishikawa, M., Hidaka, E., Ueno, I., Furihata, K., Ogiso, Y., and Katsuyama, T. A comprehensive system to explore p53 mutations. Am. J. Clin. Pathol., *110:* 368–373, 1998.
34. Summerford, C., Bartlett, J. S., and Samulski, R. J. αVβ5 integrin: a co-receptor for adeno-associated virus type 2 infection [see comments]. Nat. Med., *5:* 78–82, 1999.
35. Summerford, C., and Samulski, R. J. Membrane-associated heparan sulfate proteoglycan is a receptor for adeno-associated virus type 2 virions. J. Virol., *72:* 1438–1445, 1998.
36. Dechecchi, M. C., Tamanini, A., Bonizzato, A., and Cabrini, G. Heparan sulfate glycosaminoglycans are involved in adenovirus type 5 and 2-host cell interactions. Virology, *268:* 382–390, 2000.
37. Nemerow, G. R. Cell receptors involved in adenovirus entry. Virology, *274:* 1–4, 2000.
38. Siprashvili, Z., Sozzi, G., Barnes, L. D., McCue, P., Robinson, A. K., Eryomin, V., Sard, L., Tagliabue, E., Greco, A., Fusetti, L., Schwartz, G., Pierotti, M. A., Croce, C. M., and Huebner, K. Replacement of Fhit in cancer cells suppresses tumorigenicity. Proc. Natl. Acad. Sci. USA, *94:* 13771–13776, 1997.
39. Werner, N. S., Siprashvili, Z., Fong, L. Y., Marquitan, G., Schroder, J. K., Bardenheuer, W., Seeber, S., Huebner, K., Schutte, J., and Opalka, B. Differential susceptibility of renal carcinoma cell lines to tumor suppression by exogenous Fhit expression. Cancer Res., *60:* 2780–2785, 2000.
40. Aoki, K., Yoshida, T., Sugimura, T., and Terada, M. Liposome-mediated *in vivo* gene transfer of antisense K-ras construct inhibits pancreatic tumor dissemination in the murine peritoneal cavity. Cancer Res., *55:* 3810–3816, 1995.
41. Ohta, M., Inoue, H., Cotticelli, M. G., Kastury, K., Baffa, R., Palazzo, J., Siprashvili, Z., Mori, M., McCue, P., Druck, T., *et al.* The *FHIT* gene, spanning the chromosome 3p14.2 fragile site and renal carcinoma-associated t(3;8) breakpoint, is abnormal in digestive tract cancers. Cell, *84:* 587–597, 1996.
42. Costantini, P., Jacotot, E., Decaudin, D., and Kroemer, G. Mitochondrion as a novel target of anticancer chemotherapy. J. Natl. Cancer Inst., *92:* 1042–1053, 2000.
43. Reed, J. C. Mechanisms of apoptosis avoidance in cancer. Curr. Opin. Oncol., *11:* 68–75, 1999.
44. Bold, R. J., Termuhlen, P. M., and McConkey, D. J. Apoptosis, cancer and cancer therapy. Surg. Oncol., *6:* 133–142, 1997.
45. Jaattela, M. Escaping cell death: survival proteins in cancer. Exp. Cell Res., *248:* 30–43, 1999.
46. Hanahan, D., and Weinberg, R. A. The hallmarks of cancer. Cell, *100:* 57–70, 2000.
47. Li, H., Zhu, H., Xu, C. J., and Yuan, J. Cleavage of BID by caspase 8 mediates the mitochondrial damage in the Fas pathway of apoptosis. Cell, *94:* 491–501, 1998.
48. Zheng, T. S., Hunot, S., Kuida, K., Momoi, T., Srinivasan, A., Nicholson, D. W., Lazebnik, Y., and Flavell, R. A. Deficiency in caspase-9 or caspase-3 induces compensatory caspase activation. Nat. Med., *6:* 1241–1247, 2000.
49. Ungefroren, H., Voss, M., Jansen, M., Roeder, C., Henne-Bruns, D., Kremer, B., and Kalthoff, H. Human pancreatic adenocarcinomas express Fas and Fas ligand yet are resistant to Fas-mediated apoptosis. Cancer Res., *58:* 1741–1749, 1998.
50. Teitz, T., Wei, T., Valentine, M. B., Vanin, E. F., Grenet, J., Valentine, V. A., Behm, F. G., Look, A. T., Lahti, J. M., and Kidd, V. J. Caspase 8 is deleted or silenced preferentially in childhood neuroblastomas with amplification of MYCN [see comments]. Nat. Med., *6:* 529–535, 2000.
51. Vile, R. G., Russell, S. J., and Lemoine, N. R. Cancer gene therapy: hard lessons and new courses. Gene Ther., *7:* 2–8, 2000.
52. Koeberl, D. D., Alexander, I. E., Halbert, C. L., Russell, D. W., and Miller, A. D. Persistent expression of human clotting factor IX from mouse liver after i.v. injection of adeno-associated virus vectors. Proc. Natl. Acad. Sci. USA, *94:* 1426–1431, 1997.
53. Alexander, I. E., Russell, D. W., and Miller, A. D. DNA-damaging agents greatly increase the transduction of nondividing cells by adeno-associated virus vectors. J. Virol., *68:* 8282–8287, 1994.
54. Kornek, G. V., Schratter-Sehn, A., Marczell, A., Depisch, D., Karner, J., Krauss, G., Haider, K., Kwasny, W., Locker, G., and Scheithauer, W. Treatment of unresectable, locally advanced pancreatic adenocarcinoma with combined radiochemotherapy with 5-fluorouracil, leucovorin and cisplatin. Br. J. Cancer, *82:* 98–103, 2000.

Downloaded from http://aacrjournals.org/cancerres/article-pdf/61/12/4827/2486769/4827.pdf by guest on 24 August 2022